ISSN 1590-8844
International Journal of Mechanics and Control, Vol. 16, No. 01, 2015

OPTIMAL DESIGN OF A NEW SPHERICAL PARALLEL MANIPULATOR USED AS MASTER DEVICE

Houssem Saafi Med Amine Laribi Marc Arsicault Said Zeghloul

Dept.of GMSC, Pprime Institute

CNRS - University of Poitiers - ENSMA - UPR 3346, France

ABSTRACT

This paper deals with the optimization of a New Spherical Parallel Manipulator (N_SPM). The N_SPM is obtained by changing the kinematic of one leg of a classic spherical parallel manipulator. This change is carried out to reduce the presence of the singularity in the useful area of the workspace. The mobility of the N_SPM is similar to the classic one. First, the less-singular working mode of the N_SPM was identified then an optimization of the dexterity is made to eliminate the singularity from the useful workspace. Finally, the optimal N_SPM is presented.

Keywords: Spherical Parallel Manipulator; Optimization; Workspace; Dexterity; Genetic Algorithm.

1 INTRODUCTION

In the recent years, parallel manipulators still widely popular. They are used in many domains such as industry [1], research [2] and medicine [3]. The main advantages of parallel manipulators are their high stiffness, their high accuracy and their load capability.

The spherical parallel manipulators (SPMs) are a class of parallel manipulator that gives three degrees of freedom of rotations. They are composed of three identical legs with three revolute joints. The main application of the SPMs is orienting device such as minimally invasive surgery master device [4, 5] and camera orienting device [6, 7].

Parallel manipulators performances depend on their geometric parameters. An optimization process is needed to choose the optimal geometry for each specific application. In [4], a SPM is optimized for a MIS application. The self-rotation was not considered in the optimization process. This generates the presence of singularity in the SPM workspace for some values of the self-rotation.

In this paper we try to solve the problem of the singularity.

Contact author: Said Zeghloul

said.zeghloul@univ-poitiers.fr.

A kinematic modification of the SPM was carried out to reduce the presence of the singularity. The New SPM (N_SPM) is then optimized to eliminate the singularity from the prescribed workspace and to improve the dexterity distribution.

The paper is organized as follows. In section 2, an evaluation of the classic SPM is shown. In Section 3, the new structure of the SPM is presented. A comparative study was made in section 4 to choose the less-singular assembly mode of the N_SPM. Section 5 discusses an optimization of the N_SPM. Finally, Section 6 summarizes this paper.

2 EVALEATION OF THE CALSSIC SPM

The SPM (Fig. 1) was developed as a part of a tele-operation system to control a surgical robot. The target application is the minimally invasive surgery (MIS). In a previous work [4], the workspace of the MIS was studied to identify its size.

The SPM has three identical legs, each leg is made of two links and three revolute joints, see Fig. 2. All axes of the revolute joints are intersecting in one common point, called CoR (Centre of Rotation). Each link is characterized by the angle between its two revolute joints, as shown in Fig. 3.

This angle is constant and it represents the dimension of the link. The angle, α, characterizes the first link size and the angle, β, the second link size. The angle, γ, defines the orientation of the axis z of the platform with respect to the last joint axis. The actuated joint axes are located along an orthogonal frame.

Figure 1 Master device of a tele-operation system.

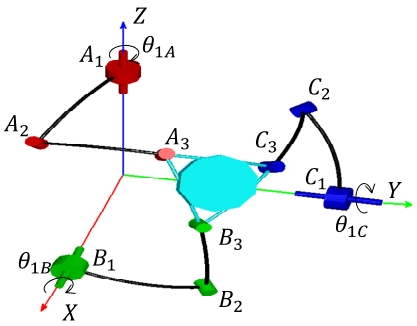

Figure 2 Spherical parallel manipulator kinematic.

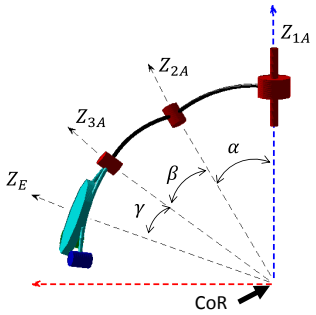

Figure 3 Kinematic of the leg A.

The orientation of the SPM is described by the Euler angles (ψ, θ, φ). The workspace of the SPM can be identified by its inverse model. The inverse model is solved using equation (1) for leg K (K=A, B and C).

$$Z_{2K}Z_{3K} = \cos(\beta) \tag{1}$$

With

$$\begin{cases} Z_{2K} = R_Z(\theta_{1K})R_X(\alpha)Z \\ Z_{3K} = R_Z(\psi)R_X(\theta)R_Z(\varphi)R_X(\gamma)Z \end{cases} \tag{2}$$

After substitution, the equation (1) leads to the following three scalar equations:

$$A_j \cos(\theta_{1K}) + B_j \sin(\theta_{1K}) = C_j; j \in \{1,2,3\} \tag{3}$$

Where A_j, B_j and C_j are coefficients that depend on the parameters (α, β, γ) and the variation of the platform given by the Euler angles (ψ, θ, φ).

Equation 3 has a solution if and only if the following constraints CD_j are respected:

$$CD_j(\alpha,\beta,\gamma,\psi,\theta,\varphi): \frac{C_j^2}{A_j^2 + B_j^2} \le 1 \tag{4}$$

These three conditions are used to identify the workspace size of the spherical parallel manipulator (SPM) and called as the orientation power function, which indicates if the arm j is able to reach the given orientation or not. The Jacobian matrix of the SPM can be written by differentiating Equation 1:

$$\dot{Z}_{2K}Z_{3K} + Z_{2K}\dot{Z}_{3K} = 0 \tag{5}$$

where,

$$\begin{cases} \dot{Z}_{2K} = \dot{\theta}_{1K}Z_{1K} \times Z_{2K} \\ \dot{Z}_{3K} = \omega \times Z_{3K} \end{cases} \tag{6}$$

with, × is the cross product and ω is the angular velocity of the end-effector.

$$\omega = \begin{bmatrix} \dot{\theta}\cos(\psi) + \dot{\varphi}\sin(\theta)\sin(\psi) \\ \dot{\theta}\sin(\psi) - \dot{\varphi}\sin(\theta)\cos(\psi) \\ \dot{\psi} + \cos(\theta) \end{bmatrix} \tag{7}$$

Equation 4 becomes:

$$\dot{\theta}_{1K}(Z_{1K} \times Z_{2K}) \cdot Z_{3K} = \omega \cdot Z_{2K} \times Z_{3K} \tag{8}$$

Indeed, we can write equation (9) in matrix form as:

$$A \cdot \omega = B \cdot \dot{\theta} \tag{9}$$

$$\omega = J \cdot \dot{\theta} \tag{10}$$

where, $\dot{\theta} = \left[\dot{\theta}_{1A}, \dot{\theta}_{1B}, \dot{\theta}_{1C}\right]^T$ is the vector of actuated joint velocities and J is the Jacobian matrix of the SPM defined as follows:

$$J = A^{-1}B \tag{11}$$

Matrix A is a 3x3 matrix and it is defined as follows:

$$A = \left[Z_{3A} \times Z_{2A} \quad Z_{3B} \times Z_{2B} \quad Z_{3C} \times Z_{2C}\right]^T \tag{12}$$

Matrix B is a diagonal 3x3 matrix and it is defined as follows:

$$B = diag[Z_{1A}(Z_{2A} \times Z_{3A}); Z_{1B}(Z_{2B} \times Z_{3B}); \\ ...Z_{1C}(Z_{2C} \times Z_{3C})] \tag{13}$$

Dexterity is a measure reflecting the error amplification due to the kinematic and statistic transformations between the joints and Cartesian space. The dexterity, $\eta(J)$, is

measured using the inverse of the condition number, *κ(J)*, of the Jacobian matrix [8], see Eq. 14.

$$\eta(J)=\frac{1}{\kappa(J)} \qquad \text{With } \kappa(J)=\|J\|\cdot\|J^{-1}\| \tag{14}$$

In previous work [4], the SPM was optimized in order to have a compact structure with a maximum of dexterity. The resulting structure is defined by the following vector of optimal design parameters:

$$I_{SPM}=[\alpha,\beta,\gamma]^T=[39.4°,34.1°,18.2°]^T$$

However a simplifying assumption was considered in this SPM optimization procedure, only a constant value for the self-rotation, $\varphi=\pi/10$, is considered. For other values of φ, the kinematic behaviour of the robot is deteriorated. Fig. 4 presents the dexterity distribution of the SPM for $\varphi=50°$ and shows the presence of the singularity inside the workspace (the singular are in dark red).

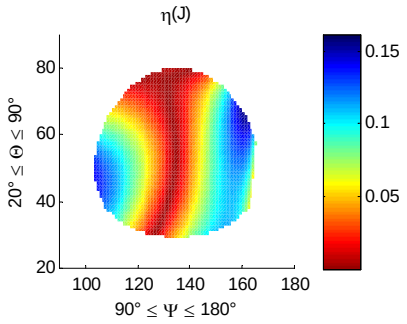

Figure 4 The dexterity distribution of the SPM over the useful workspace for φ=50° (singular area in dark red).

3 SOLVING THE SINGULARITY PROBLEM

In a previous work [9], a solution avoiding the singularity problem was proposed. This solution is based on the use of a redundant actuator without changing the design of the SPM. It was proved that the use of the redundant actuator eliminates the presence of singularity inside the workspace. However, this solution increases the weight of the end-effector. Consequently, it's not well suitable. In this present work, we propose a solution with a design change. The kinematic of only one leg is replaced. The new structure of the SPM is presented in Fig. 5.

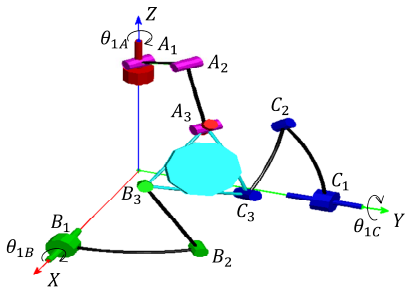

Figure 5 Kinematic structure of the new SPM.

The legs B and C are not changed and described by the same geometric parameters, [α, β, γ], as the classic SPM. The RRR kinematic structure of leg A was replaced by URU structure as illustrated in Fig 6 (R for Revolute joint and U for Universal joint). The links of the new leg have the same length, L.

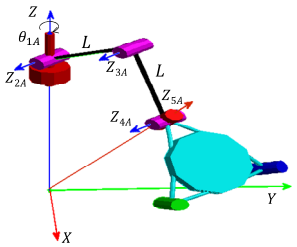

Figure 6 New kinematic of the leg A.

In order to obtain the Jacobian matrix of the new SPM, we should express the relationship between the angular velocity of the platform ω and the actuated joint velocities, $\dot{\theta}_{1A}$, $\dot{\theta}_{1B}$ and $\dot{\theta}_{1C}$.

For the legs B and C, the equation (8) is applicable. For the new leg A, we can write

$$\omega=\dot{\theta}_{1A}Z_{1A}+\dot{\theta}_{2A}Z_{2A}+\dot{\theta}_{3A}Z_{3A}+\dot{\theta}_{4A}Z_{4A}+\dot{\theta}_{5A}Z_{5A} \tag{15}$$

The reciprocal screw is used to eliminate all passive joint velocities $\dot{\theta}_{2A}$, $\dot{\theta}_{3A}$, $\dot{\theta}_{4A}$ and $\dot{\theta}_{5A}$ from equation (15) and defined as follows:

$$\$_{1A}^{r}=Z_{4A}\times Z_{5A} \tag{16}$$

This vector is perpendicular in all configurations to the vectors Z_{2A}, Z_{3A}, Z_{4A} and Z_{5A}. We multiply equation (16) by the reciprocal screw:

$$\$_{1A}^{r}\cdot\omega=\$_{1A}^{r}\cdot\dot{\theta}_{1A}Z_{1A} \tag{17}$$

$$Z_{4A}\times Z_{5A}\cdot\omega=\dot{\theta}_{1A}\cdot Z_{1A}\cdot(Z_{4A}\times Z_{5A}) \tag{18}$$

The matrices *A* and *B* become:

$$A=\begin{bmatrix}Z_{4A}\times Z_{5A} & Z_{3B}\times Z_{2B} & Z_{3C}\times Z_{2C}\end{bmatrix}^T \tag{19}$$

$$B=diag[Z_{1A}(Z_{4A}\times Z_{5A});Z_{1B}(Z_{2B}\times Z_{3B});\ldots Z_{1C}(Z_{2C}\times Z_{3C})] \tag{20}$$

4 THE LESS SINGULAR WORKING MODE OF N_SPM

If we consider the new leg, the new SPM has eight solutions (Working Modes (W.Ms)) to the inverse kinematic model. The new leg has no effect on the kinematic behavior of the N_SPM. So we consider only four working modes presented in Fig. 7. Each one of these working modes has a different behavior inside the useful workspace. The aim of this section is to identify the most suitable working mode in term of kinematic behavior. An equivalent study was made for the classic SPM in [10].

In this section, we consider that the dimensions of legs B and C are identical to those of the classic SPM (see Section II). An optimization problem will be performed in the next section in order to identify the optimal dimensions.

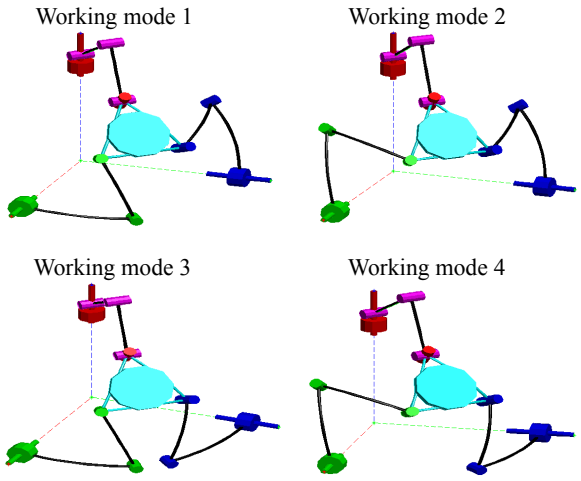

Figure 7 Working modes of the N_SPM.

For the considered parallel structure, the change of working mode is possible only through a serial singularity, when one of the two spherical legs B or C is extended or folded on in itself. This is possible only in the border of the workspace.

Figures 8, 9 and 10 show the dexterity distribution and the singularity location in the useful workspace for φ=0°, φ=50° and φ=-50° respectively.

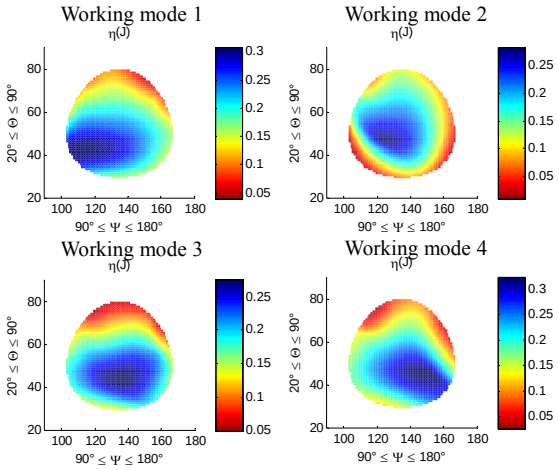

Figure 8 The dexterity distribution for the all W.Ms (φ=0°).

The singular configurations for all working modes are located on the borders of the workspace for φ=0°. However, we note that the W.Ms 1 and 4 do not present a maximum of the dexterity at the center of the workspace, unlike the W.Ms 2 and 3.

For φ=50°, the W.M. 4 presents the most suitable distribution of the dexterity. There is no singular configurations inside the workspace.

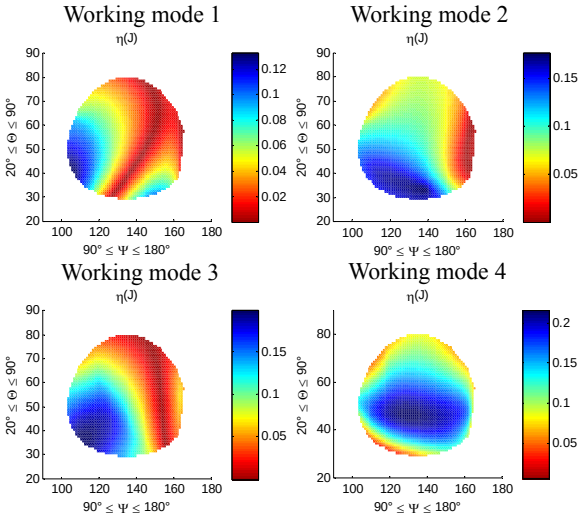

Figure 9 The dexterity distribution for the all W.Ms (φ=50°).

For φ=-50°, only W.M. 1 doesn't contain any singular configuration in the workspace. Working mode 2 contains a small singularity area in the left border of the workspace. Figures 8, 9 and 10 show that the W.M. 2 is the less singular working mode. In order to prove this observation, we propose to calculate the minimum distance, rmin, between the singularity location and the useful workspace center $O_0(\psi_0, \theta_0)$ (see Fig. 11).

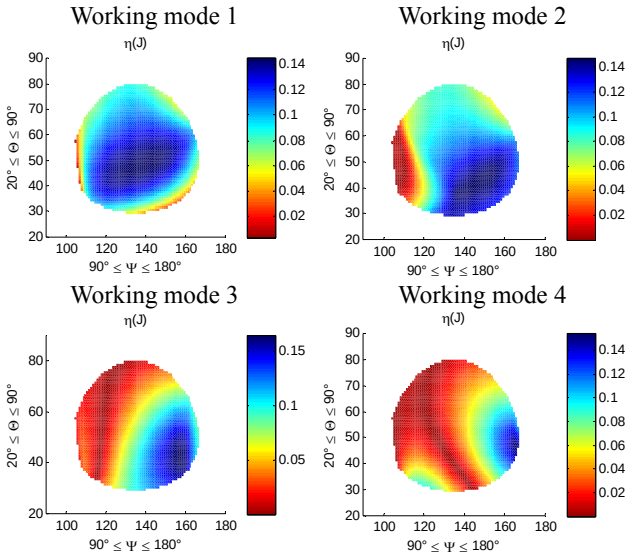

Figure 10 The dexterity distribution for the all W.Ms (φ=-50°).

This distance is calculated as follows:

$$r_{\min} = \min(r_i) = \min(\sqrt{(\psi_0 - \psi_i)^2 + (\theta_0 - \theta_i)^2} \quad (21)$$

The N_SPM is considered in singular configuration if the dexterity value is less than 0.02.

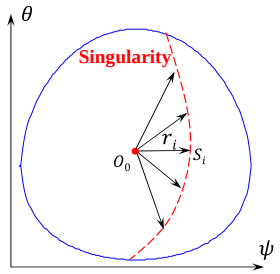

Figure 11 Minimum distance identification between the singularity and the useful workspace center, O_0.

Fig. 12 shows the evolution of r_{min} with respect to the self-rotation of the plateform. We can observe that the singularity locations are close to the border of the workspace for all considered self-rotation values. Therefore the assembly mode 2 is the less-singular assembly mode. This mode is then chosen.

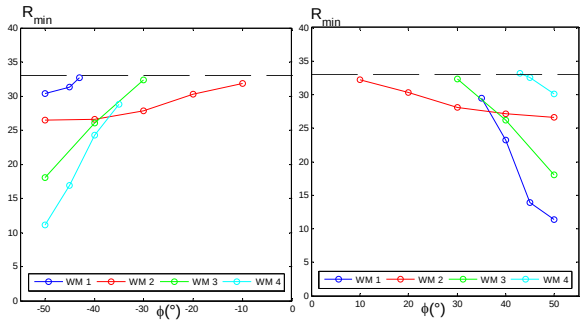

Figure 12 R_min evolution with respect to the self-rotation of the platform.

The symmetry of the architecture presented by the working mode 2 (see Fig. 7) has leads to a symmetric kinematic behavior. Due to this symmetry, the following study will focus only on values of the self-rotation between 0° and 50°.

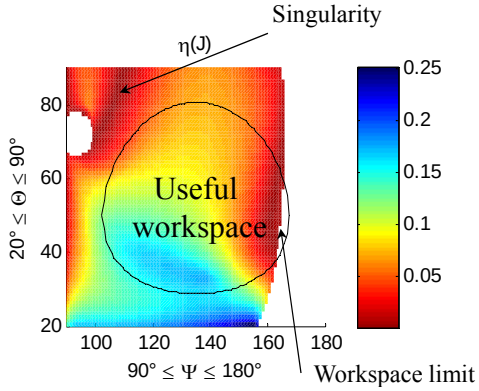

Figure 13 The dexterity destribution for the W.M. 2 (φ=50°).

In addition of the presence of the singularity for φ=-50° and φ=50°, the workspace size does not fit the needed workspace, see Fig. 13. To solve this problem, we propose to optimize the parameters of the N_SPM in order improve the workspace size and to eliminate the presence of singularity.

4 OPTIMIZATION OF THE N_SPM

In this section, the dexterity was considered as a criterion to determine the link dimensions of the optimal new SPM. The link dimensions are defined by the design vector I=[α,β,γ]. The performance is evaluated over a workspace free of singularity, which is specified as a cone with an apex angle equal to 26°. This represents the dimensional characteristic of the prescribed workspace.

Since the singularities are located at the border of the workspace, only the workspace boundary is considered in order to simplify the optimization process. The workspace border is discretized by 100 points as illustrated on Fig. 14.

The proposed approach is based on the minimization of an objective function F(I) subjected to two constraints. The first constraint concerns the workspace and aims to guarantee that the N_SPM workspace fits the prescribed one for the self-rotation φ between 0° and 50°. The second constraint concerns the Jacobian matrix conditioning to guarantee dexterous workspace (free of singularity) for φ between 0° and 50°.

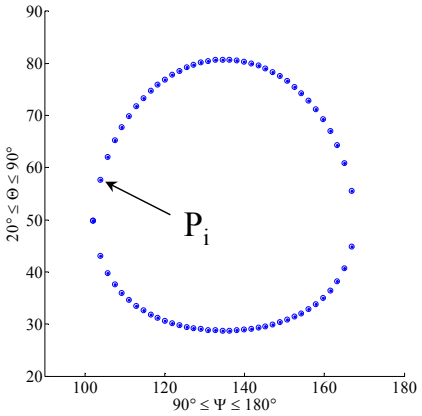

Figure 14 Prescribed workspace border in (θ, ψ) plane and discretized on N=100 points.

The optimization problem can be then formulated as follows:

minimize: $F(I) = \sum_{i}^{N} \kappa(I, P_i, \varphi = 0°) + \sum_{i}^{N} \kappa(I, P_i, \varphi = 50°)$

subject to:

1- $CD_j(\alpha, \beta, \gamma, \psi, \theta, \varphi) : \dfrac{C_j^2}{A_j^2 + B_j^2} \le 1$

2- $\kappa(I, P_i) < \kappa_{\max}$

3- $x_{lb} \le x \le x_{up}; \quad x \in \{\alpha, \beta, \gamma\}$

where *F(I)* is the objective function defined as a sum of the condition number value for all points *Pi* for φ=0° and φ=50°, x_{lb} and x_{up}, are the lower and upper bounds of the variables *x* given in Table 1 respectively, and κ_{max} represents the maximum permissible value for the condition number which is considered equal to 25 in the optimization process.

Table I - The lower and upper bounds of the design variables *x*

	α[deg]	β[deg]	γ[deg]
x_{lb}	35	30	16
x_{up}	50	45	20

A genetic algorithm (GA) is used to solve the optimization problem, because of its robustness and simplicity. Initially the algorithm generates 500 sets of different design parameters as the first parent generation. Then the three standard genetic operations (reproduction, crossover, and mutation) are performed to produce a new generation. Such procedures are repeated until the maximum number of generations is achieved, or the required accuracy is satisfied.
The optimal design vector of the resulted structure is given in table 2. Fig. 15 shows the Optimal N_SPM.

Table II - OPTIMAL SOLUTION.

Design vector	Variables			κ_{max}
	α[deg]	β[deg]	γ[deg]	
I_{nSPM}	49.5	39.1	16.1	25

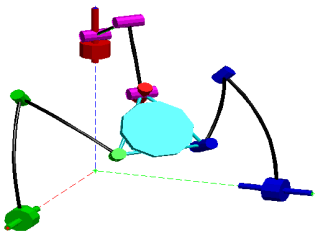

Figure 15 Optimal N_SPM.

The dimension of the new kinematic leg is defined by the parameter *L* calculated using the following equation:

$$L = R\frac{\sin(\theta_{2A}^{MAX})}{2} \tag{22}$$

where, R is the SPM radius, $\theta_{2A}^{MAX} = \theta^{MAX} + \delta - \gamma$ the maximum angle between Z_{1A} and Z_{5A} and δ is the security angle chosen to be equal to 2° in order to avoid the serial singularity of the leg A.
The dexterity distributions for the resulted structure for φ=0°, φ=50° and φ=-50° are shown in Fig. 16.

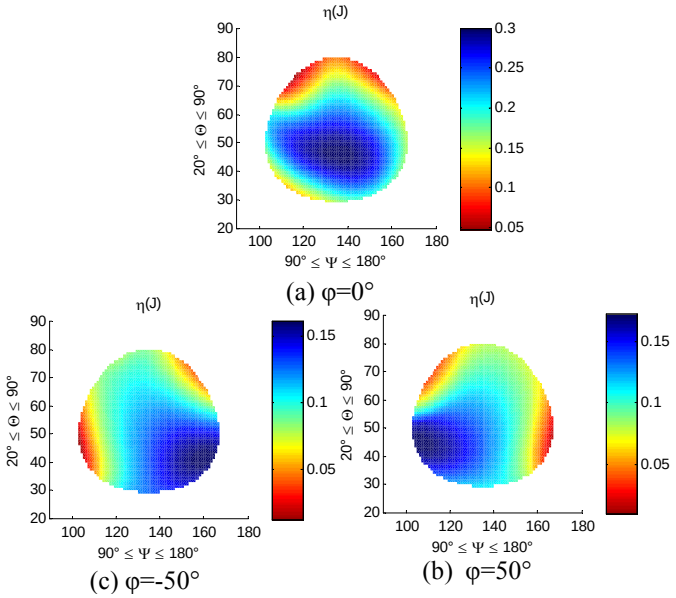

Figure 16 Dexterity distribution for the optimal N_SPM.

We can observe first, that the robot workspace fits the prescribed workspace for φ between -50° and 50°, which means that the robot is able to reach all the orientations needed to achieve the surgical task. Second, the obtained workspace is free-singular for φ between -50° and 50°.

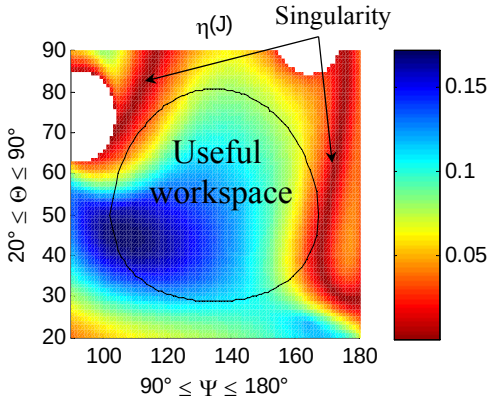

Figure 17 Dexterity distribution for the optimal N_SPM for the whole workspace(φ=50°).

Fig. 17 shows the singularity area of the optimal N_SPM for φ=50°. We can observe that the singularity is outside the useful workspace.
Fig. 18 shows a 3d printed prototype of the optimal N_SPM. This prototype was made to validate the functioning of the N_SPM. It is made of ABS and its size is about the third of the size of the master device presented in Fig. 1.

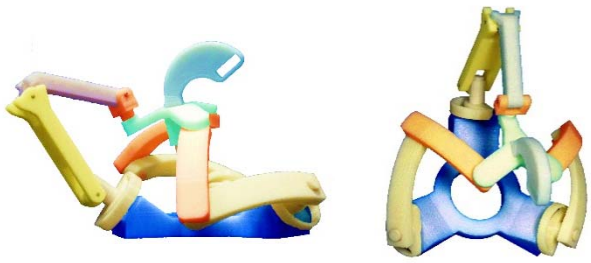

Figure 18 Prototype of the optimal SPM.

6 CONCLUSION

An optimization of a new spherical parallel manipulator (N_SPM) was presented in this work. The objective of this optimization is to obtain a new SPM with a workspace overlaying the prescribed workspace without presence of the singularity. First, the singularity problem of the classic SPM was shown. Second, a new architecture of the spherical parallel manipulator was presented. Then, the less-singular assembly mode of the new SPM was identified and selected. Finally, an optimization based on the dexterity and subject to the workspace size and the presence of singularity is made to improve the kinematic behaviour of the N_SPM.

ACKNOWLEDGMENT

This research is supported by the Poitou-Charentes region 2007-2013 (program project 10 Images and interactivities), in partnership with the European Union (FEDER/ERDF, European Regional Development Fund) and by ROBOTEX, the French national network of robotics platforms (N° ANR-10-EQPX-44-01).

REFERENCES

[1] S. M. Wang and K. F. Ehmann, "Error Model and Accuracy Analysis of a Six-Dof Stewart Platform," ASME Journal of Manufacturing Science and Engineering, Vol. 124, No. 2, 2002, pp. 286-295. doi: 10.1115/1.1445148

[2] J. Wang, C. Wu and X. J. Liu, "Performance Evaluation of Parallel Manipulators: Motion/Force Transmissibility and Its Index," Mechanism and Machine Theory, Vol. 45, No. 10, 2010, pp. 1462-1476.

[3] Saafi, H.; Laribi, M.A.; Zeghloul, S.; Ibrahim, M.Y., "Development of a spherical parallel manipulator as a haptic device for a tele-operation system: Application to robotic surgery," Industrial Electronics Society, IECON 2013 - 39th Annual Conference of the IEEE, vol., no., pp. 4097-4102, 10-13 Nov. 2013.

[4] A. Chaker, A. Mlika, M. A. Laribi, L. Romdhane and S. Zeghoul, "Synthesis of a Spherical Parallel Manipulator for a Dexterous Medical Task", Front. Mech. Eng. 2012, Volume 7, Number 2, pp. 150-162, doi: 10.1007/s11465-012-0325-4.

[5] A. Ma, S. Payandeh, Analysis and experimentation of a 4-dof haptic device, in: Haptic interfaces for virtual environment and teleoperator systems, 2008, pp. 351-356. doi: 10.1109/HAPTICS.2008.4479970.

[6] L. Birglen, C. Gosselin, N. Pouliot, B. Monsarrat, T. Laliberte, Shade, a new 3-dof haptic device, Robotics and Automation, IEEE Transactions on 18 (2) (2002), pp. 166–175. doi: 10.1109/TRA.2002.999645.

[7] C. Gosselin, E. St.Pierre, M. Gagne, On the development of the agile eye, Robotics Automation Magazine, IEEE 3(4), 1996, pp. 29–37. doi: 10.1109/100.556480.

[8] C. Gosselin, J. Angeles, "A Global Performance Index for the Kinematic Optimisation of Robotic Manipulators", ASME Journal of Mechanical Design, vol.113, n° 3, pp. 220-226, 1991.

[9] Saafi, H.; Laribi, M.A.; Zeghloul, S.; "Redundantly actuated 3-RRR spherical parallel manipulator used as a haptic device: improving dexterity and eliminating singularity", 22nd international conference on robotics in Alpe-Adria-Danube region, Portoroz, Slovenia, 11-13 September 2013.

[10] Saafi, H.; Laribi, M.A.; Zeghloul, S.; "Less-Singular Assembly-Mode for 3-RRR Spherical Parallel Manipulator", 3rd IFToMM International Symposium on Robotics and Mechatronics, 2-4 October 2013, Singapore.